

Changing climate both increases and decreases European river floods

*Original*

Changing climate both increases and decreases European river floods / Blöschl, Günter; Hall, Julia; Viglione, Alberto; Perdigão, Rui A P; Parajka, Juraj; Merz, Bruno; Lun, David; Arheimer, Berit; Aronica, Giuseppe T; Bilibashi, Ardian; Bohá, Milo; Bonacci, Ognjen; Borga, Marco; anjevac, Ivan; Castellarin, Attilio; Chirico, Giovanni B; Claps, Pierluigi; Frolova, Natalia; Ganora, Daniele; Gorbachova, Liudmyla; Gül, Ali; Hannaford, Jamie; Harrigan, Shaun; Kireeva, Maria; Kiss, Andrea; Kjeldsen, Thomas R; Kohnová, Silvia; Koskela, Jarkko J; Ledvinka, Ondrej; Macdonald, Neil; Mavrova-Guirquinova, Maria; Mediero, Luis; Merz, Ralf; Molnar, Peter; Montanari, Alberto; Murphy, Conor; Osuch, Marzena; Ovscharuk, Valeria; Radevski, Ivan; Salinas, José I; Sauquet, Eric; Šraj, Mojca; Szolgay, Jan; Volpi, Elena; Wilson, Donna; Zaimi, Klodian; Zivkovi, Nežad. - In: NATURE. - ISSN 0028-0836. - (2019). [10.1038/s41586-019-1495-6]

*Publisher:*

Springer Nature Publishing

*Published*

DOI:10.1038/s41586-019-1495-6

*Terms of use:*

This article is made available under terms and conditions as specified in the corresponding bibliographic description in the repository

*Publisher copyright*

(Article begins on next page)



# Changing climate both increases and decreases European river floods

Günter Blöschl<sup>1†</sup>, Julia Hall<sup>1†</sup>, Alberto Viglione<sup>1, 12</sup>, Rui A. P. Perdigão<sup>1</sup>, Juraj Parajka<sup>1</sup>, Bruno Merz<sup>2</sup>, David Lun<sup>1</sup>, Berit Arheimer<sup>3</sup>, Giuseppe T. Aronica<sup>4</sup>, Ardian Bilibashi<sup>5</sup>, Miloň Boháč<sup>6</sup>, Ognjen Bonacci<sup>7</sup>, Marco Borga<sup>8</sup>, Ivan Čanjevac<sup>9</sup>, Attilio Castellarin<sup>10</sup>, Giovanni B. Chirico<sup>11</sup>, Pierluigi Claps<sup>12</sup>, Natalia Frolova<sup>13</sup>, Daniele Ganora<sup>12</sup>, Liudmyla Gorbachova<sup>14</sup>, Ali Gül<sup>15</sup>, Jamie Hannaford<sup>16</sup>, Shaun Harrigan<sup>17</sup>, Maria Kireeva<sup>13</sup>, Andrea Kiss<sup>1</sup>, Thomas R. Kjeldsen<sup>18</sup>, Silvia Kohnová<sup>19</sup>, Jarkko J. Koskela<sup>20</sup>, Ondrej Ledvinka<sup>6</sup>, Neil Macdonald<sup>21</sup>, Maria Mavrova-Guirguinova<sup>22</sup>, Luis Mediero<sup>23</sup>, Ralf Merz<sup>24</sup>, Peter Molnar<sup>25</sup>, Alberto Montanari<sup>9</sup>, Conor Murphy<sup>26</sup>, Marzena Osuch<sup>27</sup>, Valeryia Ovcharuk<sup>28</sup>, Ivan Radevski<sup>29</sup>, José L. Salinas<sup>1</sup>, Eric Sauquet<sup>30</sup>, Mojca Šraj<sup>31</sup>, Jan Szolgay<sup>18</sup>, Elena Volpi<sup>32</sup>, Donna Wilson<sup>33</sup>, Klodian Zaimi<sup>34</sup>, and Nenad Živković<sup>35</sup>

<sup>1</sup>Institute of Hydraulic Engineering and Water Resources Management, Technische Universität Wien, Vienna, Austria

<sup>2</sup>Helmholtz Centre Potsdam, GFZ German Research Centre for Geosciences, Potsdam, Germany

<sup>3</sup>Swedish Meteorological and Hydrological Institute, Norrköping, Sweden

<sup>4</sup>Department of Engineering, University of Messina, Messina, Italy

<sup>5</sup>CSE – Control Systems Engineer, Renewable Energy Systems & Technology, Tirana, Albania

<sup>6</sup>Czech Hydrometeorological Institute, Prague, Czechia

<sup>7</sup>Faculty of Civil Engineering, Architecture and Geodesy, Split University, Split, Croatia

<sup>8</sup>Department of Land, Environment, Agriculture and Forestry, University of Padova, Padua, Italy

<sup>9</sup>University of Zagreb, Faculty of Science, Department of Geography, Zagreb, Croatia

<sup>10</sup>Department of Civil, Chemical, Environmental and Materials Engineering (DICAM), Università di Bologna, Bologna, Italy

<sup>11</sup>Department of Agricultural Sciences, University of Naples Federico II, Naples, Italy

<sup>12</sup>Department of Environment, Land and Infrastructure Engineering (DIATI), Politecnico di Torino, Turin, Italy

<sup>13</sup>Department of Land Hydrology, Lomonosov Moscow State University, Moscow, Russia

<sup>14</sup>Department of Hydrological Research, Ukrainian Hydrometeorological Institute, Kiev, Ukraine

<sup>15</sup>Department of Civil Engineering, Dokuz Eylül University, Izmir, Turkey

<sup>16</sup>Centre for Ecology & Hydrology, Wallingford, Oxfordshire, UK

<sup>17</sup>Forecast Department, European Centre for Medium-Range Weather Forecasts (ECMWF), UK

<sup>18</sup>Department of Architecture and Civil Engineering, University of Bath, Bath, UK

<sup>19</sup>Slovak University of Technology in Bratislava, Faculty of Civil Engineering, Department of Land and Water Resources Management, Bratislava, Slovakia

<sup>20</sup>Finnish Environment Institute, Helsinki, Finland

<sup>21</sup>Department of Geography and Planning & Institute of Risk and Uncertainty, University of Liverpool, Liverpool, UK

<sup>22</sup>University of Architecture, Civil Engineering and Geodesy, Sofia, Bulgaria

<sup>23</sup>Department of Civil Engineering: Hydraulic, Energy and Environment, Universidad Politécnica de Madrid, Madrid, Spain

<sup>24</sup>Department for Catchment Hydrology, Helmholtz Centre for Environmental Research – UFZ, Halle, Germany

<sup>25</sup>Institute of Environmental Engineering, ETH Zurich, Zurich, Switzerland

<sup>26</sup>Irish Climate Analysis and Research Units (ICARUS), Department of Geography, Maynooth University, Ireland

<sup>27</sup>Department of Hydrology and Hydrodynamics, Institute of Geophysics Polish Academy of Sciences, Warsaw, Poland

<sup>28</sup>Hydrometeorological Institute, Odessa State Environmental University, Odessa, Ukraine

<sup>29</sup>Institute of Geography, Faculty of Natural Sciences and Mathematics, Ss. Cyril and Methodius University, Skopje, Republic of Macedonia

<sup>30</sup>Irstea, UR RiverLy, Lyon-Villeurbanne, France

<sup>31</sup>University of Ljubljana, Faculty of Civil and Geodetic Engineering, Ljubljana, Slovenia

<sup>32</sup>Department of Engineering, University Roma Tre, Rome, Italy

<sup>33</sup>Norwegian Water Resources and Energy Directorate, Oslo, Norway

<sup>34</sup>Institute of Geo-Sciences, Energy, Water and Environment (IGEWE), Polytechnic University of Tirana, Tirana, Albania

<sup>35</sup>University of Belgrade, Faculty of Geography, Belgrade, Serbia

\* e-mail: bloeschl@hydro.tuwien.ac.at

† These authors contributed equally to this work.

1 **Abstract**

2  
3 **Climate change has led to concerns of increasing river floods resulting from the greater water**  
4 **holding capacity of a warmer atmosphere<sup>1</sup>. This concern is reinforced by evidence of**  
5 **increasing economic losses in many parts of the world, including Europe<sup>2</sup>. Any changes in**  
6 **river floods would have lasting implications for designing flood protection measures and for**  
7 **flood risk zoning. Existing studies have been unable to identify a consistent continental-scale**  
8 **climatic change signal in flood discharge observations in Europe<sup>3</sup>, because of limited spatial**  
9 **coverage and choices in the grouping of hydrometric stations. Here we show that clear**  
10 **regional patterns of both increases and decreases in observed river flood discharges in the last**  
11 **five decades in Europe are evident, which are likely manifestations of a changing climate. Our**  
12 **results suggest that (i) increasing autumn and winter rainfall has led to increasing floods in**  
13 **northwestern Europe, (ii) decreasing precipitation and increasing evaporation have led to**  
14 **decreasing floods in medium and large catchments in southern Europe and (iii) decreasing**  
15 **snowcover and snowmelt as a result of warmer temperatures have led to decreasing floods in**  
16 **eastern Europe. Regional flood discharge trends in Europe range from an increase of +11.4%**  
17 **per decade to a decrease of -23.1%. Notwithstanding the spatial and temporal heterogeneity**  
18 **of the observational record, the flood changes identified here are broadly consistent with**  
19 **climate model projections for the next century<sup>4,5</sup>, suggesting that climate-driven changes are**  
20 **already happening, which supports calls for future climate change consideration in flood risk**  
21 **management.**  
22

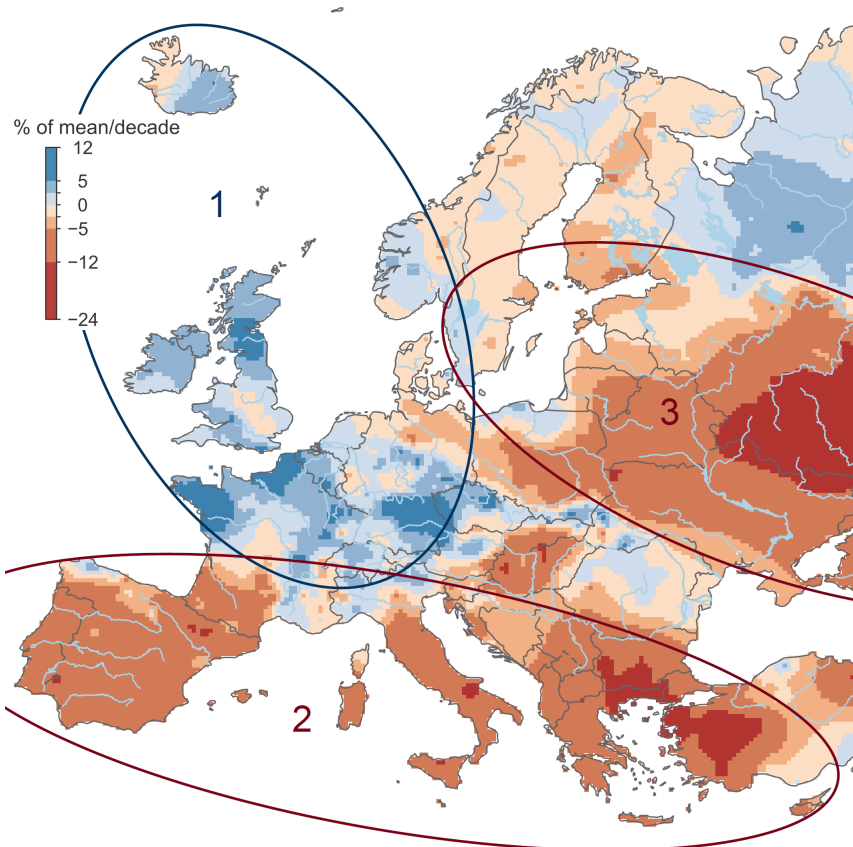
23 River floods are among the most costly natural hazards. Global annual average losses are estimated  
24 at US \$104 billion<sup>6</sup>, and are expected to increase as a result of economic growth, urbanization and  
25 climatic change<sup>2,7</sup>. Physical arguments of increased heavy precipitation resulting from the enhanced  
26 water holding capacity in a warmer atmosphere and the occurrence of numerous large floods have  
27 exacerbated concerns of increasing flood magnitudes<sup>1</sup>. However, observations of individual extreme  
28 events do not necessarily imply that the long-term statistics of flood discharge are also increasing<sup>3</sup>.

29  
30 In Europe, a climatic change signal in flood discharges over the past five decades has been  
31 demonstrated in relation to changes in timing of floods within the year<sup>8</sup>. For example, in  
32 northeastern Europe, warmer air temperatures have led to earlier spring snowmelt floods. However,  
33 changes in flood discharges are still contested, as no coherent large-scale observational evidence  
34 has to date been available at the continental scale, as a result of limited spatial coverage and choices  
35 in the grouping of hydrometric stations<sup>3</sup>. A number of studies point towards increases in flood  
36 discharges in western Europe in the past five decades. The findings include upward trends in flood  
37 discharges in 15% of the stations<sup>9</sup>, an increase in the occurrence of extreme flood discharges by  
38 44%<sup>10</sup>, and significant increases in major-flood occurrence in medium sized catchments<sup>11</sup>. However,  
39 these studies are not fully representative as the stations are mainly clustered around western Europe.

40  
41 Here we analyze the most comprehensive data set of flood observations in Europe<sup>12</sup> to show that a  
42 changing climate has increased river flood discharges in some regions of Europe, but decreased  
43 floods in others. We base our analysis on river discharge observations from 3738 gauging stations  
44 for the period 1960–2010. The catchment areas range between 5 and 100,000 km<sup>2</sup>. For each station,  
45 we extracted a series consisting of the highest peak discharge recorded in each calendar year, the  
46 annual maximum peak flow. We estimated the trend in each series using the Theil-Sen slope  
47 estimator, tested the statistical significance with the Mann-Kendall test, and estimated regional  
48 trends by spatial interpolation. We also derived the long-term evolution of floods using a 10-year  
49 moving average filter. Finally, we analyzed in a similar fashion the change signal of three plausible  
50 drivers of floods: annual maximum 7-day precipitation; highest monthly soil moisture in each year;  
51 and spring (January to April) mean air temperature as a proxy for snowmelt and snowfall-to-rain  
52 transition. We examined the consistency of the changes in the drivers with those of the floods by  
53 comparing the change patterns and by Spearman rank correlation coefficients.

54  
55 Our data show a clear regional pattern in flood trends across Europe (Fig. 1). Regional trends,  
56 relative to the mean flood discharges over 1960–2010, range from an increase of +11.4% to a  
57 decrease of -23.1% per decade (Fig. 1). The uncertainties of the regional trends (Extended Data Fig.  
58 2b) are small (typically between 1 and 2% per decade) relative to the spatial signal. Local trends  
59 (Extended Data Fig. 2a) at the stations range from an increase of +17.8% to a decrease of -28.8% of  
60 the long-term station mean per decade. The spatial patterns of trends are grouped into three main  
61 regions. In northwestern Europe (Fig. 1, region 1), ~69% of stations show an increasing flood trend  
62 (Extended Data Table 2a) with an average local increase of +2.3% per decade. In southern Europe  
63 (Fig. 1, region 2), ~74% of stations show a decreasing trend with a regional average trend of -5%  
64 per decade. In eastern Europe (Fig. 1, region 3), ~78% of stations show a decreasing flood trend  
65 with an average decrease of -6% per decade. In northern Scandinavia and northwestern Russia,  
66 trends are less pronounced.

67

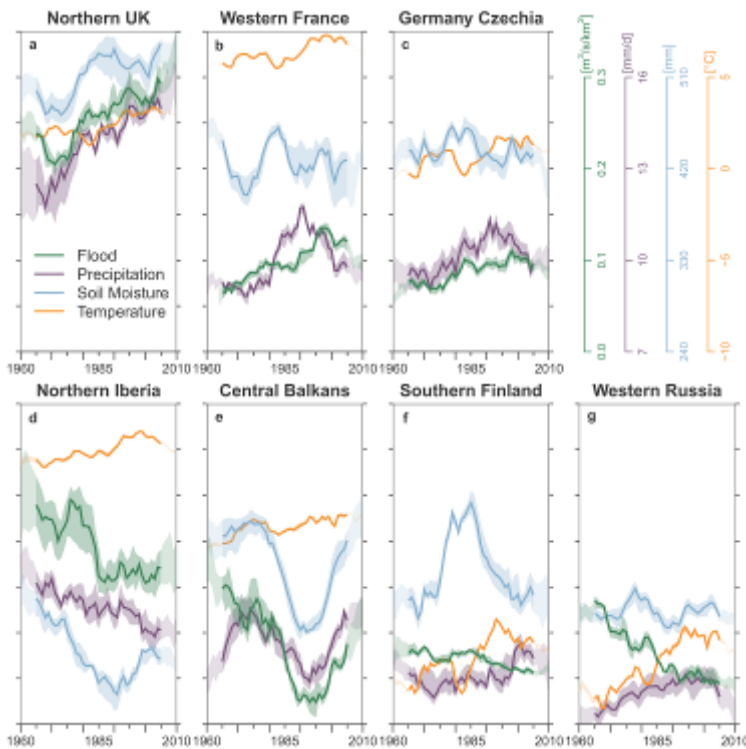


68  
 69 **Fig. 1 | Observed regional trends of river flood discharges in Europe (1960–2010).** Blue  
 70 indicates increasing flood discharges, red decreasing flood discharges (percentage change per  
 71 decade of the mean annual flood discharge). No. 1–3 indicate regions with distinct drivers: [1]  
 72 northwestern Europe: increasing rainfall and soil moisture; [2] southern Europe: decreasing rainfall  
 73 and increasing evaporation; [3] eastern Europe: decreasing and earlier snowmelt. The trends are  
 74 based on  $n = 2370$  hydrometric stations. For uncertainties see Extended Data Fig. 2b.

75  
 76  
 77 To interpret these changes we focused on seven hotspots of change, where flood trends are  
 78 particularly clear and flood processes are broadly similar<sup>8</sup> (Extended Data Fig. 2). Because floods  
 79 result from the interaction between precipitation, soil moisture and snowmelt, we analyzed the  
 80 temporal evolution of these drivers, using air temperature as a surrogate for snowmelt, and  
 81 compared them to that of floods (Extended Data Fig. 4 a–g). Depending on the region, some of  
 82 these drivers can be more important than others in explaining flood changes<sup>8</sup>.

83  
 84 In northern UK, floods predominantly result from winter rains associated with high soil moisture<sup>14</sup>  
 85 (Extended Data Fig. 4a). The increase in the flood discharges therefore closely follows increases in  
 86 winter rainfall and to some degree that of soil moisture (Fig. 2a). This is also shown by statistically  
 87 significant positive correlations between the temporal variability of flood discharges and these two  
 88 drivers (Spearman rank correlation coefficient  $r = 0.70$  and  $0.36$ , respectively, Table 1). In western  
 89 France (Fig. 2b), southern Germany and western Czechia (Fig. 2c), increases in floods are also  
 90 associated with increases in rainfall, although the correlation with soil moisture is stronger than in  
 91 the UK, reflecting the important role of soil moisture in flood generation during spring and  
 92 summer<sup>15</sup> (Extended Data Fig. 4 a–c). In northern Iberia (Fig. 2d), decreasing floods are mainly  
 93 caused by decreasing winter rainfall, amplified by decreasing soil moisture linked to increasing  
 94 evapotranspiration<sup>16</sup>. Similarly, in the central Balkans (Fig. 2e), floods have decreased over most of  
 95 the study period as a result of decreasing precipitation and soil moisture, but the trend appears to  
 96 have reversed in the 1990s. In southern Finland (Fig. 2f) and western Russia (Fig. 2g), floods  
 97 usually occur in spring<sup>17</sup>, and snowmelt plays an important role. The data show that air temperature

98 has strongly increased (more than 0.5°C per decade) and spring and early summer flood discharges  
 99 have decreased ( $r = -0.34$  and  $-0.55$ , respectively, Table 1), reflecting shallower snow packs, earlier  
 100 spring thaw (Extended Data Fig. 4f-g), and decreasing snowmelt.  
 101



102  
 103 **Fig. 2 | Long-term temporal evolution of flood discharges and their drivers for seven hotspots**  
 104 **in Europe.** (a) Northern UK, (b) Western France (c) Southern Germany and Western Czechia, (d)  
 105 Northern Iberia, (e) Central Balkans, (f) Southern Finland, (g) Western Russia. Observed floods  
 106 (green), maximum 7-day precipitation (purple), maximum monthly soil moisture (blue), and mean  
 107 spring air temperature (orange). Solid lines show the median and shaded bands indicate the spatial  
 108 variability within the hotspots (25<sup>th</sup> and 75<sup>th</sup> percentile). All data were subjected to a 10-year  
 109 moving average filter. Vertical axes are indicated in top right corner.  
 110  
 111

112 **Table 1 | Spearman's rank correlation coefficient ( $r$ ) between hotspot medians of the annual**  
 113 **series of flood discharge and their drivers.** Confidence bounds of  $r$  are given in Extended Data  
 114 Table 2b.

	Northern UK	Western France	Germany Czechia	Northern Iberia	Central Balkans	Southern Finland	Western Russia
Precipitation	<b>0.70</b> **	0.41 *	0.40 *	<b>0.54</b> **	0.22	0.08	-0.13
Soil Moisture	0.36 *	<b>0.57</b> **	<b>0.56</b> **	0.37 *	<b>0.68</b> **	0.20	0.30
Spring temperature	0.09 †	0.50 ** †	0.04	0.02	-0.29	<b>-0.34</b>	<b>-0.55</b> **

115 [(\*\*)  $p$ -value < 0.001, (\*)  $p$ -value < 0.01, † Little snow influence on floods. Bold print indicates largest correlation  
 116 coefficients in each hotspot.]  
 117

118 In northwestern Europe (Fig. 1, region 1), increases in extreme precipitation (Fig. 2a-c; Extended  
 119 Data Fig. 5b) are related to the poleward shift of the subpolar jet and associated storm tracks  
 120 observed since the 1970s associated with more prevalent positive phases of the North Atlantic  
 121 Oscillation (NAO) and polar warming<sup>18</sup>. The relationship of NAO variability with polar warming is  
 122 still debated. Floods in the northern UK hotspot are closely aligned with increasing precipitation  
 123 resulting in a mean flood discharge trend of +6.6% (Extended Data Table 2c).  
 124

125 In southern Europe (Fig. 1, region 2), the northward shift of the subtropical jet and associated storm  
126 tracks<sup>19</sup> as a result of the expansion of the Hadley cell<sup>20</sup> has led to decreasing precipitation, which,  
127 together with increasing evapotranspiration<sup>16</sup> related to warmer temperatures, has substantially  
128 reduced soil moisture by around 5% per decade (Extended Data Figs. 5b,6b,7b). The combined  
129 effect has resulted in decreasing flood discharges in the catchments analyzed here. Small  
130 catchments of a few square kilometers are not contained in the data set (the median catchment size  
131 of region 2 is about 400 km<sup>2</sup>), as they are usually not monitored or the flood series are too short for  
132 trend analyses. In small catchments, local short-duration convective storms with high intensities are  
133 more relevant for flood generation than long-duration synoptic storms, which produce floods in  
134 medium and large catchments contained in the data<sup>21</sup>. Local convective storms are expected to  
135 increase in a warmer climate<sup>22</sup>, which means that floods in small catchments may have actually  
136 increased. Additionally, soil compaction, abandoned terraces and land-cover changes may increase  
137 flood discharges in small catchments<sup>23</sup>. The difference in catchment size may explain the apparent  
138 inconsistency between the occurrence of numerous floods in small catchments in recent years in  
139 southern Europe<sup>21</sup> and the decreasing trend in Fig. 1.

140  
141 In all but southern Europe, increases in extreme precipitation (Fig. 2a–c,f,g; Extended Data Fig. 5b)  
142 are related to increased atmospheric blocking associated with decreasing pressure differences  
143 between Greenland and the Baltic, which has decreased the speed of zonal (west-east) flow and  
144 increased the chance of standing planetary waves<sup>24</sup>. However, it is only in northwestern Europe (Fig.  
145 1, region 1), where the increase in extreme precipitation is reflected in increased flood discharges,  
146 as winter storms in that region cause winter floods<sup>8</sup>. Further in the east, snowmelt is more relevant  
147 for flood generation.

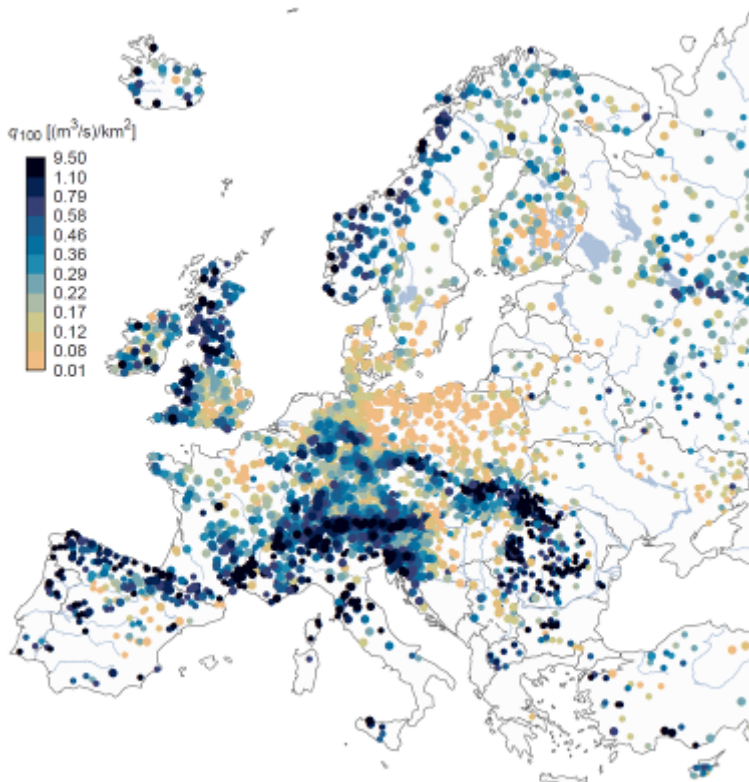
148  
149 In eastern Europe, spring air temperature has increased by as much as 1°C per decade (Extended  
150 Data Fig. 6b). This has resulted in much less extensive spring snow cover<sup>25</sup>, a shift of snowfall to  
151 rainfall when air temperatures are around zero, shallower snow packs, earlier snowmelt<sup>8</sup>, likely  
152 increased infiltration resulting from shallower freezing depths and therefore smaller floods, even  
153 though extreme precipitation in summer has increased<sup>26</sup>. The mean flood trend in the western  
154 Russian hotspot is -18.2% (Extended Data Table 2c). Given the colder background temperature  
155 (Extended Data Fig. 6a) and larger snowpack in northwestern Russia, the increasing temperatures  
156 are not yet changing snowmelt patterns, and hence not decreasing floods (Fig. 1).

157  
158 While past studies have focused on a few catchments or were clustered around western Europe<sup>9–11,27</sup>,  
159 this study provides a continental perspective, which allows for an analysis of climate processes that  
160 manifest themselves at larger scales. Isolated local or national scale studies, however, are broadly  
161 consistent with our findings.

162  
163 Our results have implications for flood risk management in medium and large sized catchments.  
164 The trends shown in Fig. 1 are estimates of changes in the mean annual flood. Since mean annual  
165 floods and more extreme floods are usually closely correlated<sup>28</sup>, similar trends could also be  
166 expected for the 100-year flood, which is often the key design criterion in flood risk management.  
167 In northwest Europe (Fig. 1, region 1), flood discharges per unit catchment area (specific flood  
168 discharges) are generally high (Fig. 3). For example, on the west coast of the British-Irish Isles and  
169 Norway, the specific 100-year flood discharge during the period 1960-2010 was ~0.9 (m<sup>3</sup>/s)/km<sup>2</sup>  
170 (Fig. 3), with floods increasing by ~5% per decade. However, in eastern Europe (Fig 1, region 3),  
171 specific flood discharges are rather small (Fig. 3), and are likely to become smaller in a changing  
172 climate. For example, in the Baltic countries, southern Poland and the Ukraine, the 100-year flood  
173 of ~0.1 (m<sup>3</sup>/s)/km<sup>2</sup> would decrease to ~0.075 (m<sup>3</sup>/s)/km<sup>2</sup> if the observed decrease of ~5% per decade  
174 persists over the next 50 years. In southern Europe, even if flood discharges decrease in medium  
175 and large catchments, discharges are still generally high (Fig. 3), as a result of the proximity to the



176 Mediterranean Sea and associated heavy precipitation events<sup>29</sup>. Floods in small catchments may  
177 actually increase as a result of enhanced convective storms<sup>30</sup> and land-use change<sup>23</sup>.  
178  
179



180  
181 **Fig. 3 | Specific 100-year floods ((m<sup>3</sup>/s)/km<sup>2</sup>) in Europe**, where larger points indicate 90%  
182 confidence intervals smaller than 60% of the estimate.  
183

184 Increasing flood discharges imply that, the 100-year flood discharge five decades ago, now has a  
185 smaller return period than 100 years, i.e. that discharge is likely to be exceeded on average more  
186 often than once in 100 years. In northwestern Europe, what was the 100-year flood discharge in  
187 1960 has now typically become a 50- to 80-year flood discharge (Extended Data Fig. 8), which will  
188 make flood defense structures less safe. In eastern Europe, the 100-year flood discharge has now  
189 become a 125- to 250-year flood discharge, which will make structures less economical. While  
190 Extended Data Fig. 8, and Fig. 3, do provide a continental overview, they do not replace  
191 national-scale and local studies where more detailed information may be available.  
192

193 It should be noted that the flood trends observed here do not necessarily extrapolate into the future  
194 as they may be related to climate variability rather than persistent changes in time<sup>11</sup>. Also, the trends  
195 depend on the observation period<sup>3</sup>, so may differ if the observation period is extended. However,  
196 the regions with a distinct climatic change signal in observed flood discharges identified here are  
197 broadly coherent with the projected flood changes in Europe. Most projections for the end of the  
198 21<sup>st</sup> century suggest increasing floods in (north)western Europe due to increasing precipitation, and  
199 decreasing floods in eastern and northern Europe due to increasing temperatures<sup>4,5</sup>. This means that  
200 changes in flood discharge magnitudes are already underway, which adds credence to those  
201 projections and supports the need to account for climate induced changes in flood risk management.  
202  
203

#### 204 **References:**

- 205 1. IPCC. *Managing the Risks of Extreme Events and Disasters to Advance Climate Change*  
206 *Adaptation. A Special Report of Working Groups I and II of the Intergovernmental Panel on*

- 207 *Climate Change*. (Cambridge University Press, Cambridge, UK and New York, NY, USA,  
208 2012).
- 209 2. EASAC. European Academies' Science Advisory Council Statement; Extreme weather events  
210 in Europe - Preparing for climate change adaptation: an update on EASAC's 2013 study. at  
211 <<https://easac.eu/publications/details/extreme-weather-events-in-europe/>>
- 212 3. Hall, J. *et al.* Understanding flood regime changes in Europe: a state of the art assessment.  
213 *Hydrol. Earth Syst. Sc.* **18**, 2735–2772 (2014).
- 214 4. Kundzewicz, Z. *et al.* Differences in flood hazard projections in Europe-their causes and  
215 consequences for decision making. *Hydrol. Sci. J.* **62**, 1–14 (2017).
- 216 5. Thober, S. *et al.* Multi-model ensemble projections of European river floods and high flows at  
217 1.5, 2, and 3 degrees global warming. *Environ. Res. Lett.* **13**, 014003 (2018).
- 218 6. UNISDR. *Making Development Sustainable: The Future of Disaster Risk Management. Global*  
219 *Assessment Report on Disaster Risk Reduction*. (Geneva, Switzerland: United Nations  
220 International Strategy for Disaster Reduction (UNISDR), 2015).
- 221 7. Winsemius, H. C. *et al.* Global drivers of future river flood risk. *Nat. Clim. Chang.* **6**, 381–385  
222 (2016).
- 223 8. Blöschl, G. *et al.* Changing climate shifts timing of European floods. *Science* **357**, 588–590  
224 (2017).
- 225 9. Mangini, W. *et al.* Detection of trends in magnitude and frequency of flood peaks across  
226 Europe. *Hydrol. Sci. J.* **63**, 493–512 (2018).
- 227 10. Berghuijs, W., Aalbers, E., Larsen, J., Trancoso, R. & Woods, R. Recent changes in extreme  
228 floods across multiple continents. *Environ. Res. Lett.* **12**, (2017).
- 229 11. Hodgkins, G. A. *et al.* Climate-driven variability in the occurrence of major floods across North  
230 America and Europe. *J. Hydrol.* **552**, 704–717 (2017).
- 231 12. Hall, J. *et al.* A European Flood Database: facilitating comprehensive flood research beyond  
232 administrative boundaries. *Proc. Int. Assoc. Hydrol. Sci.* **370**, 89–95 (2015).
- 233 13. Sivapalan, M., Blöschl, G., Merz, R. & Gutknecht, D. Linking flood frequency to long-term  
234 water balance: Incorporating effects of seasonality. *Water Resour. Res.* **41**, W06012 (2005).
- 235 14. Bayliss, A. C. & Jones, R. C. *Peaks-over-threshold flood database: Summary statistics and*  
236 *seasonality. IH Report No. 121*. (Institute of Hydrology, Wallingford, UK, 1993).
- 237 15. Schröter, K., Kunz, M., Elmer, F., Mühr, B. & Merz, B. What made the June 2013 flood in  
238 Germany an exceptional event? A hydro-meteorological evaluation. *Hydrol. Earth Syst. Sc.* **19**,  
239 309–327 (2015).
- 240 16. Mediero, L., Santillán, D., Garrote, L. & Granados, A. Detection and attribution of trends in  
241 magnitude, frequency and timing of floods in Spain. *J. Hydrol.* **517**, 1072–1088 (2014).
- 242 17. Hall, J. & Blöschl, G. Spatial patterns and characteristics of flood seasonality in Europe.  
243 *Hydrol. Earth Syst. Sc.* **22**, 3883–3901 (2018).
- 244 18. IPCC. *2013: Climate Change 2013: The Physical Science Basis. Contribution of Working*  
245 *Group I to the Fifth Assessment Report of the Intergovernmental Panel on Climate Change*.  
246 (Cambridge University Press, Cambridge, UK and New York, USA, 2013).
- 247 19. Archer, C. L. & Caldeira, K. Historical trends in the jet streams. *Geophys. Res. Lett.* **35**, (2008).
- 248 20. Kang, S. M. & Lu, J. Expansion of the Hadley cell under global warming: Winter versus  
249 summer. *J. Clim.* **25**, 8387–8393 (2012).
- 250 21. Amponsah, W. *et al.* Integrated high-resolution dataset of high-intensity European and  
251 Mediterranean flash floods. *Earth Syst. Sci. Data* **10**, 1783–1794 (2018).
- 252 22. Ban, N., Schmidli, J. & Schär, C. Heavy precipitation in a changing climate: Does short-term  
253 summer precipitation increase faster? *Geophys. Res. Lett.* **42**, 1165–1172 (2015).
- 254 23. Rogger, M. *et al.* Land-use change impacts on floods at the catchment scale - Challenges and  
255 opportunities for future research. *Water Resour. Res.* **53**, 5209–5219 (2017).
- 256 24. Perdigão, R. A. P., Pires, C. A. L. & Hall, J. Synergistic Dynamic Theory of Complex  
257 Coevolutionary Systems: Disentangling Nonlinear Spatiotemporal Controls on Precipitation.  
258 *arXiv:1611.03403 [math.DS]* (2016).

- 259 25. Estilow, T. W., Young, A. H. & Robinson, D. A. A long-term Northern Hemisphere snow cover  
260 extent data record for climate studies and monitoring. *Earth Syst. Sci. Data* **7**, 137–142 (2015).
- 261 26. Frolova, N. L. *et al.* Hydrological hazards in Russia: origin, classification, changes and risk  
262 assessment. *Nat. Hazards* **88**, 103–131 (2017).
- 263 27. Mediero, L. *et al.* Identification of coherent flood regions across Europe by using the longest  
264 streamflow records. *J. Hydrol.* **528**, 341–360 (2015).
- 265 28. Salinas, J. L., Castellarin, A., Kohnova, S. & Kjeldsen, T. Regional parent flood frequency  
266 distributions in Europe-Part 2: Climate and scale controls. *Hydrol. Earth Syst. Sc.* **18**, 4391–  
267 4401 (2014).
- 268 29. Xoplaki, E., Gonzalez-Rouco, J. F., Luterbacher, J. & Wanner, H. Wet season Mediterranean  
269 precipitation variability: influence of large-scale dynamics and trends. *Clim. Dynam.* **23**, 63–78  
270 (2004).
- 271 30. Brooks, H. E. Severe thunderstorms and climate change. *Atmos. Res.* **123**, 129–138 (2013).
- 272

273 **Methods**

274 **Data sets**

275 The hydrological data used in this study were obtained from a newly created European Flood  
276 Database<sup>12</sup>, with subsequent updates, containing data from 3738 hydrometric gauging stations from  
277 68 European data sources for the period 1960 to 2010 (Extended Data Table 1). Choice of the study  
278 period was guided by a tradeoff between data availability in terms of record length and spatial  
279 coverage. The database consists of the highest discharge (daily mean or instantaneous discharge) in  
280 each calendar year for each station. For consistency, we chose to analyze the annual maximum  
281 flood rather than multiple floods within a year in all stations, as in many areas only annual maxima  
282 were available. The stations are located within the domain bounded by 22.25 W – 60.25 E and  
283 34.25 N – 71.25 N (Extended Data Fig. 1), and catchment areas range between 5 and 100,000 km<sup>2</sup>.

284  
285 The data set was screened for data errors, and catchments that were known, or were identified, to  
286 have experienced strong human modifications such as reservoirs that could affect changes in flood  
287 discharges were excluded. The screening involved data pre-selection by co-authors and additional  
288 visual examination of the flood records in question, analysis of flood seasonality (jumps in timing  
289 and large differences to surrounding stations), and examination of the catchment area in google  
290 maps. While local human effects on the floods of individual stations cannot be excluded, the focus  
291 of this study was on regionally consistent patterns of change where such effects will not be relevant.  
292 In a few catchments, the available flood data had been corrected for the effects of reservoirs to  
293 represent near natural flood discharge. In a few cases, local reservoirs may influence the data, but  
294 this does not affect the regional pattern. The station density is rather uneven (Extended Data Fig.  
295 1b). In southern Europe it is lower as some stations were removed because of reservoir effects. In  
296 Italy, reduced record lengths are related to organizational changes of the hydrographic services<sup>12</sup>. In  
297 eastern Europe the density of available stations is generally lower than in other countries and, again,  
298 some stations were removed because of reservoir effects.

299  
300 For estimating the flood discharge trends (Fig. 1 and 2, Extended Data Fig. 2 and 8), only stations  
301 that satisfied the following three criteria were considered: at least 40 years of data were available  
302 during 1960–2010, the record started in 1968 or earlier, and ended in 2002 or later. In the countries  
303 with the highest station densities (Austria, Germany, Switzerland), only stations with at least 49  
304 years of data were included in order to obtain a more even spatial distribution across Europe. In  
305 Cyprus, Italy and Turkey, stations with at least 30 years of data were included, and in Spain 40  
306 years of data without restrictions to the start and end of the record. This selection resulted in a set of  
307 2370 stations with a median catchment size of 381 km<sup>2</sup>. Sensitivity analyses indicated that the  
308 large-scale spatial pattern of increasing and decreasing flood trends across Europe is not influenced  
309 by the choice of record length although the trend of individual stations tends to be sensitive to  
310 record length, when increasing the required record length by 5 years, the percentage of significantly  
311 positive and negative trends (Extended Data Table 2a) changes only slightly from respectively  
312 11.52% and 16.50% to 11.04% and 16.95%. In this study we evaluated linear trends of the flood  
313 discharges. Alternative models of change (e.g. step changes) could also be tested but are beyond the  
314 scope of this study.

315  
316 For each hydrometric gauging station, the contributing catchment boundary was derived from the  
317 CCM River and Catchment Database<sup>31</sup>. Daily gridded precipitation sum and mean air temperature  
318 data from the E-OBS data set (Version 17.0)<sup>32</sup> for the period 1960–2010 were used. The data  
319 consist of interpolated ground-based observations with a spatial resolution of 0.25°. Monthly  
320 gridded soil moisture data from the CPC Soil Moisture data set<sup>33</sup> for the period 1960–2010 were  
321 analyzed. The data are model-calculated monthly averaged soil moisture water-height equivalents  
322 with a spatial resolution of 0.5°.

323  
324

325 **Analysis method**

326 As a first step, we estimated the discharge trend by the Theil-Sen slope estimator<sup>34,35</sup>. The trend  
 327 estimator  $\beta$  is the median slope calculated using the differences of discharge  $Q$  over all possible  
 328 pairs of years ( $i$  and  $j$ ,  $i < j$ ) within the time series,

329 
$$\beta = \text{median}\left(\frac{Q_j - Q_i}{j - i}\right) \quad (1)$$

330 where  $\beta$  has units of m<sup>3</sup>/s per year, which was plotted as percentage of the mean flood discharge per  
 331 decade in Extended Data Fig. 2. The trends were tested for significance by the Mann-Kendall test<sup>36</sup>  
 332 (Extended Data Table 2a). Some false positives, i.e. detected trends where no trend is present,  
 333 would be expected because of the large number of stations. The Mann-Kendall test requires the  
 334 flood discharges to be temporally independent. We therefore tested whether lag 1 autocorrelation  
 335 exists in the residuals from the trends. 92% of the stations did not exhibit significant lag 1  
 336 autocorrelation at the 5% level, suggesting that the Mann-Kendall test is applicable. To identify  
 337 regional spatial patterns within Europe,  $\beta$  was spatially interpolated using the *autoKrige* function  
 338 (automatic kriging) of the R *automap* package<sup>37</sup>. The derived trend patterns are plotted in Fig. 1 and  
 339 in the background of Extended Data Fig. 2a. The uncertainty of the estimated trends at the stations  
 340 was estimated by bootstrapping<sup>40</sup> and is shown as points in Extended Data Fig. 2b. The uncertainty  
 341 of the regional trends was estimated as the block kriging standard deviation (kriging error) using the  
 342 *autoKrige* function and is shown in the background of Extended Data Fig. 2b. The variogram  
 343 estimated by the function is

344 
$$\gamma(h) = c_0 + c_1 \left(1 - \frac{1}{2^{v-1}\Gamma(v)} \left(\frac{h}{r}\right)^v K_v\left(\frac{h}{r}\right)\right) \quad (2)$$

345 where  $h$  is lag,  $c_0 = 10.061$  (%/decade)<sup>2</sup>,  $c_1 = 57.708$  (%/decade)<sup>2</sup>,  $r = 2394.4$  km,  $v = 0.2$  and  $K_v$   
 346 is the modified Bessel function of the second kind. We used block kriging rather than ordinary  
 347 kriging as we are interested in the uncertainty of the regional estimate rather than that of the local  
 348 estimate. The uncertainty is evaluated at a 200 x 200 km block size which is the scale at which we  
 349 suggest Fig. 1 and Extended Data Fig. 2a to be read.

350  
 351 In order to evaluate the robustness of the spatial trend patterns we repeated the interpolation,  
 352 however, only using stations with significant trends (Extended Data Fig. 3a). The overall pattern is  
 353 similar to that of the interpolation using all stations (Extended Data Fig. 2a). Additionally, we  
 354 repeated the interpolation but only using randomly selected stations with distances from each other  
 355 larger than 50 km to examine the effect of spatial correlations on the trends (Extended Data Fig. 3b).  
 356 Again, the patterns are similar.

357  
 358 As a second step, we selected rectangular areas or hotspots of change based on similarity of  
 359 discharge trends and average flood timing as a proxy for flood processes (Extended Data Fig. 2,  
 360 Extended Data Table 2c). We standardized the flood series of individual stations to zero mean and  
 361 unit variance to make flood changes within hotspots comparable,

362 
$$Q_{i,k}^0 = \frac{Q_{i,k} - \mu_{Q_k}}{\sigma_{Q_k}} \quad (3)$$

363 where  $\mu_{Q_k}$  and  $\sigma_{Q_k}$  are the mean and the standard deviation of station  $k$ , respectively. To compare  
 364 results between the hotspots we denormalised the flood series of each hotspot  $h$  by the mean  
 365 specific flood discharge  $\mu_h$  ((m<sup>3</sup>/s)/km<sup>2</sup>) over all years, and the square root  $\sigma_h$  of the mean  
 366 temporal variance,

367 
$$Q_{i,k}^* = \sigma_h Q_{i,k}^0 + \mu_h \quad (4)$$

368 and estimated the long-term evolution in flood discharge with a centered 10-year moving averaging  
 369 window. We plotted the median of these series within each hotspot (solid lines) and 25<sup>th</sup> and 75<sup>th</sup>  
 370 percentiles of all stations in that hotspot (shaded bands) in Fig. 2. Additionally, the original local  
 371 flood discharges were tested for significance of a general trend in each hotspot by the Regional

372 Mann-Kendall test<sup>38</sup> (Extended Data Table 2c). Names of hotspots are only indicative and do not  
373 correspond to any exactly defined geographic area.  
374

375 To investigate rain-induced effects on flood changes, we identified for each grid point of the E-OBS  
376 dataset the 7-day period with maximum precipitation in each calendar year (with at least 30 years of  
377 annual data available). Increases of spring temperatures around or below the freezing point are  
378 considered a proxy for snow accumulation, melt and the transition from snowfall to rainfall. To  
379 understand the effect of these snowmelt processes on flood discharge, we calculated mean air  
380 temperature from January to April. When soil moisture is high, even small rainstorms may produce  
381 floods. To understand the effect of high soil moisture on floods, we identified for each grid point of  
382 the CPC Soil Moisture dataset the highest monthly soil moisture in each calendar year. We repeated  
383 the trend analyses for annual maximum precipitation, spring temperature, and annual maximum  
384 monthly soil moisture (Extended Data Fig. 5–7) on a 0.5° grid.  
385

386 In the hotspot analyses, the time series for these three climate variables were extracted based on  
387 their location within the catchment boundaries (or within a buffer distance for small areas), from  
388 which Spearman's rank correlation coefficients ( $r$ ) with the spatial medians of the original flood  
389 discharge series were calculated (Table 1). Confidence bounds at the 90% confidence level of  $r$   
390 were estimated by stochastic block bootstrapping (*boot* package of R, random block size  
391 geometrically distributed with mean of 5 years) and are given in Extended Data Table 2b. The long-  
392 term evolution of the three climate variables were calculated and plotted in a similar fashion as  
393 those of the floods in Fig. 2.  
394

395 We also analysed changes in the timing of the climate indices and floods as proxies for changing  
396 flood processes using previously established methods<sup>8</sup> (Extended Data Fig. 4). The timing is used to  
397 interpret the process drivers of flood discharge changes. For Extended Data Fig. 4a, b, d the snow  
398 melt index is not shown, as it is of little relevance for flooding<sup>8</sup>.  
399

400 To evaluate the relevance of the observed flood changes for flood management, the 100-year flood  
401 ( $Q_{100}$ ) was estimated for each station using a Generalised extreme value (GEV) distribution

$$402 \quad Q_T = \xi + \frac{\eta}{\kappa} \cdot \left[ 1 - (-\ln(1 - 1/T))^{\kappa} \right] \quad (5)$$

403 where  $Q_T$  is the  $T$ -year flood discharge. The parameters  $\xi$ ,  $\eta$  and  $\kappa$  were estimated from the flood  
404 discharge series by Bayesian inference through an MCMC algorithm<sup>39</sup>. Non-informative uniform  
405 prior distributions were used for  $\xi$  and  $\log(\eta)$ , while a normal distribution consistent with the  
406 geophysical prior<sup>41</sup> were used for  $\kappa$ . 4000 parameter samples were drawn from the posterior  
407 distributions from which 4000 100-year floods were calculated for each station by Eq. (5). The  
408 median and the relative width of the 90% credible intervals are shown in Fig. 3. For comparability  
409 of the 100-year flood in catchments of different sizes, flood discharges per unit catchment area  
410 (specific flood discharges;  $q_{100} = Q_{100}/A$ , where  $A$  is catchment area) are shown.  
411

412 If flood discharges change over time, the return period  $T$  may also change, e.g., the 100-year flood  
413 may become the 10-year flood if the flood discharges increase. Change in return period was  
414 therefore estimated by allowing the parameter  $\xi$  in Eq. (5) to change with time  $t$  as

$$415 \quad \xi = a + b \cdot t \quad (6)$$

416 where the posterior distributions of  $a$ ,  $b$ ,  $\eta$  and  $\kappa$  were estimated from the flood discharge series by  
417 Bayesian inference through the same MCMC algorithm<sup>39</sup>, using non-informative uniform prior  
418 distributions for  $a$  and  $b$ . More complex models than (6) were excluded because, for most of the  
419 stations, they did not outperform (6) based on the WAIC information criterion<sup>42</sup>. 4000 parameter  
420 samples were drawn from the posterior distributions from which 4000 100-year floods in 1960 were  
421 calculated for each station by Eqs. (5) and (6) with  $t = 1960$ . The changed return period in 2010 of

422 these 4000 flood peaks were computed by inverting Eq. (5) and by Eq. (6) with  $t = 2010$ . Finally,  
423 the median of the 4000 return periods was used as the 2010 return period of the 100-year flood  
424 discharge in 1960. Those stations where the 5<sup>th</sup> and the 95<sup>th</sup> percentiles of the uncertainty  
425 distribution agreed in the sign of change, were plotted as large points in Extended Data Fig. 8 while  
426 those where this was not the case were plotted as smaller points to indicate the uncertainty involved  
427 in the estimation.

428  
429 To identify large-scale spatial patterns, the logarithms of the 2010 return periods of the 100-year  
430 flood discharge in 1960 were spatially interpolated using the *autoKrige* function<sup>37</sup> (Extended Data  
431 Fig. 8). For estimating the stationary 100-year specific flood discharge  $q_{100}$  (Eq. (5), Fig. 3), less  
432 stringent selection criteria (at least 30 years of data) than in all the other analyses were used as it  
433 can be estimated more robustly than trends and changes in the return period, which resulted in 3738  
434 stations (Extended Data Fig. 1a).

435  
436 In this paper we have analyzed flood discharge trends. The flood data set is freely available and can  
437 be used for a wide range of analyses.

438  
439

#### 440 **Data Availability**

441 The flood discharge data from the data holders/sources listed in Extended Data Table 1 that were used in this  
442 paper can be downloaded from Zenodo. The precipitation and temperature data from the E-OBS dataset can  
443 be downloaded from [www.ecad.eu/download/ensembles/ensembles.php](http://www.ecad.eu/download/ensembles/ensembles.php). The CPC soil moisture data can be  
444 downloaded from [www.esrl.noaa.gov/psd](http://www.esrl.noaa.gov/psd).

445

#### 446 **Code Availability**

447 The code for the trend and extreme value analyses can be downloaded from GitHub.

448

#### 449 **References Methods**

- 450 31. Vogt, J. *et al.* *A pan-European River and Catchment Database*. European Commission, Joint  
451 *Research Centre* (2007).
- 452 32. Haylock, M. *et al.* A European daily high-resolution gridded data set of surface temperature and  
453 precipitation for 1950-2006. *J. Geophys. Res.* **113**, (2008).
- 454 33. Van den Dool, H., Huang, J. & Fan, Y. Performance and analysis of the constructed analogue  
455 method applied to US soil moisture over 1981-2001. *J. Geophys. Res.* **108**, (2003).
- 456 34. Sen, P. K. Estimates of the Regression Coefficient Based on Kendall's Tau. *J. Am. Stat. Assoc.*  
457 **63**, 1379–1389 (1968).
- 458 35. Theil, H. A Rank-invariant Method of Linear and Polynomial Regression Analysis, Part 1.  
459 *Proc. R. Neth. Acad. Sci.* **53**, 386–392 (1950).
- 460 36. Mann, H. B. Nonparametric tests against trend. *Econometrica: Journal of the Econometric*  
461 *Society*, 245-259 (1945).
- 462 37. Hiemstra, P. H., Pebesma, E. J., Twenhöfel, C. J. & Heuvelink, G. B. Real-time automatic  
463 interpolation of ambient gamma dose rates from the Dutch radioactivity monitoring network.  
464 *Comput. Geosci.* **35**, 1711–1721 (2009).
- 465 38. Helsel, D. R. & Frans, L. M. Regional Kendall Test for Trend. *Environ. Sci. Technol.* **40**, 4066–  
466 4073 (2006).
- 467 39. Renard, B., Lang, M. & Bois, P. Statistical analysis of extreme events in a non-stationary  
468 context via a Bayesian framework: case study with peak-over-threshold data. *Stoch. Env. Res.*  
469 *Risk A.* **21**, 97–112 (2006).
- 470 40. Wilcox, R. A note on the Theil - Sen regression estimator when the regressor is random and the  
471 error term is heteroscedastic. *Biometrical Journal: Journal of Mathematical Methods in*  
472 *Biosciences*, 40(3), 261-268 (1998).
- 473 41. Martins, E. S., & Stedinger, J. R. Generalized maximum-likelihood generalized extreme-value  
474 quantile estimators for hydrologic data. *Water Resources Research*, 36(3), 737-744 . (2000).

475 42. Watanabe, S. (2010). Asymptotic equivalence of Bayes cross validation and widely applicable  
476 information criterion in singular learning theory. *Journal of Machine Learning Research*, 11,  
477 3571-3594.

478  
479

#### 480 **ACKNOWLEDGEMENTS**

481 Supported by the ERC Advanced Grant “FloodChange” project (no. 291152), the Horizon 2020  
482 ETN “System Risk” project (no 676027), the DFG “SPATE” project (FOR 2416), the FWF  
483 “SPATE” project (I 3174), and a Russian Foundation for Basic Research (RFBR) project (no. 17-  
484 05-41030 rgo\_a). The data analysis was performed in R using the supporting packages *automap*,  
485 *boot*, *lattice*, *maptools*, *ncdf4*, *plyr*, *raster*, *RColorBrewer*, *rgdal* and *rworldmap*. The authors also  
486 acknowledge the involvement in the data screening process of C. Álvaro Díaz, I. Borzi, E.  
487 Diamantini, K. Jeneiová, M. Kupfersberger, S. Mallucci and S. Persiano during their stays at the  
488 Vienna University of Technology. We thank L. Gaál and D. Rosbjerg for contacting Finnish and  
489 Danish data holders, respectively; B. Renard (France), W. Rigott (South Tyrol, Italy), G. Lindström  
490 (Sweden) and P. Burlando (Switzerland) for assistance in preparing and/or providing data or  
491 metadata from their respective regions. We acknowledge all flood data providers listed in Extended  
492 Data Table 1.

493

#### 494 **Author contributions**

495 G.B. and J.H. designed the study and wrote the first draft of the paper. G.B. initiated the study.  
496 J.H. collated the database with the help of most of the co-authors, and conducted the analyses.  
497 A.V. conducted the MCMC analysis. G.B., J.H., A.V., R.P., J.P. and B.M. interpreted the results in  
498 the context of underlying geophysical mechanisms. J.P. compiled the catchment boundaries.  
499 D.L. contributed to the statistical analysis. M.B., I.Č., A.K., S.K., O.L., M.M.-G., R.M., P.M., I.R.,  
500 J.L.S., J.S. and N.Ž. interpreted the results in central Europe. G.T.A., A.B., O.B., M.B., A.C.,  
501 G.B.C., P.C., D.G., A.M., L.M., M.Š., E.V. and K.Z. interpreted the results in southern Europe.  
502 B.A., J.J.K. and D.W. interpreted the results in northern Europe. J.H., S.H., T.R.K., N.M., C.M. and  
503 E.S. interpreted the results in western Europe. N.F., L.G., A.G., M.K., M.O. and V.O. interpreted  
504 the results in eastern Europe. All authors contributed to framing and revising the paper.

505

506 **Competing interests** The authors declare no competing interests.

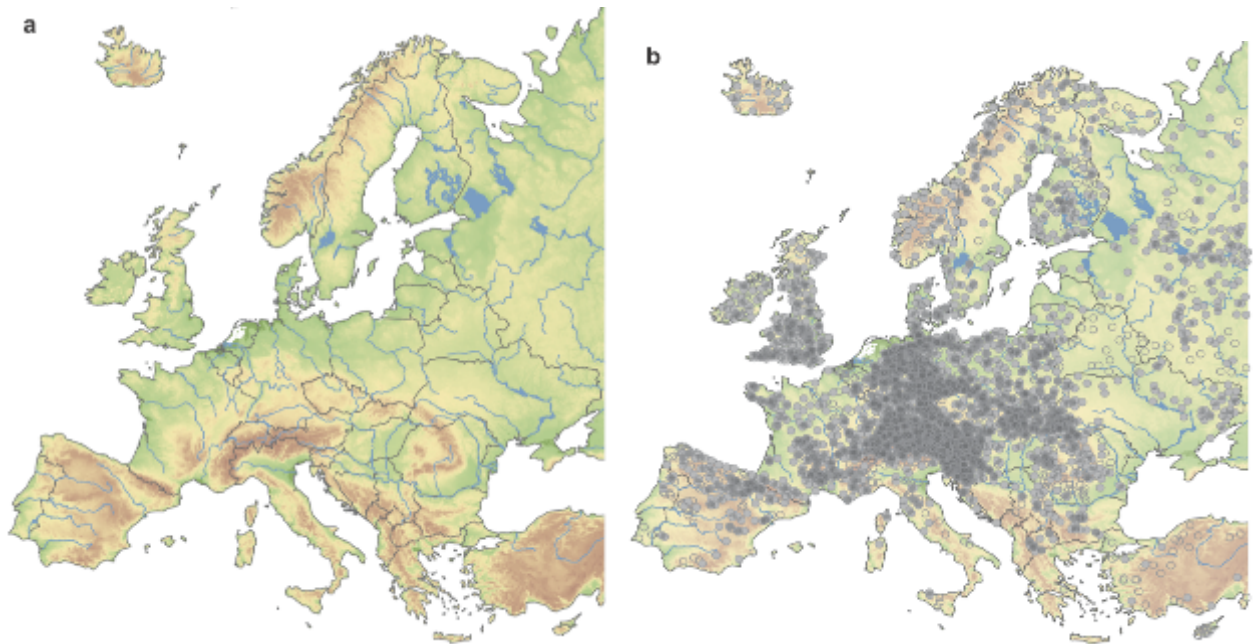
507 **Correspondence** should be addressed to G.B. (bloeschl@hydro.tuwien.ac.at)

508



509 **Extended Data display items**

510



511

512

513

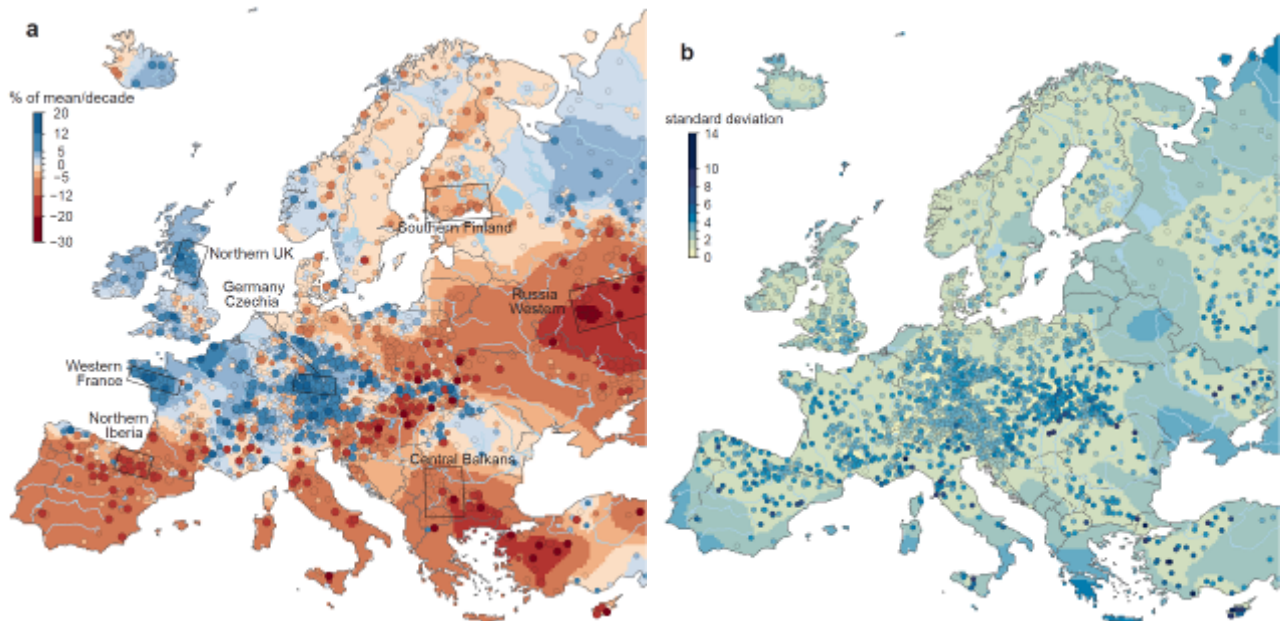
514

515

516

517

**Extended Data Figure 1 | Map of European study area.** (a) Elevation, main rivers and lakes and (b) location of the hydrometric stations analyzed. Open and full circles indicate stations with  $\geq 30$  years ( $n = 3738$ ) and  $\geq 40$  years ( $n = 2835$ ) of flood discharge data, respectively.



518

519

520

521

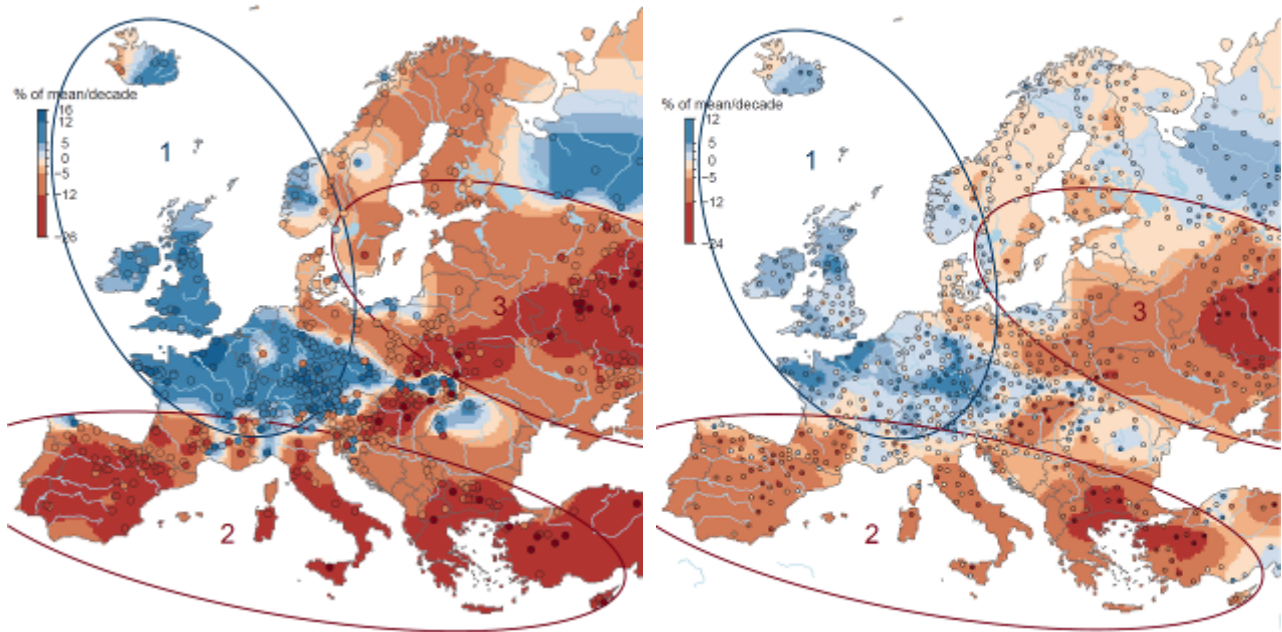
522

523

524

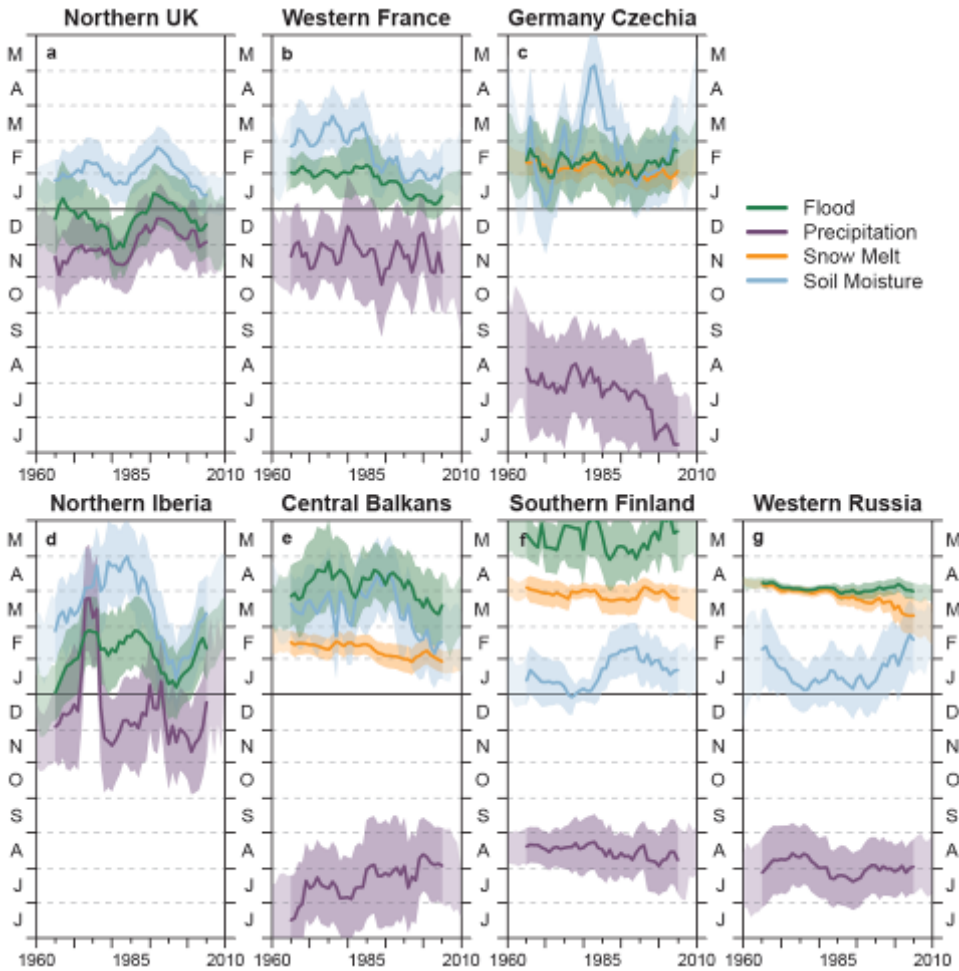
525

**Extended Data Figure 2 | Observed trends of river flood discharges in Europe (1960–2010).** (a) Points show local trends ( $n = 2370$ ), where larger points indicate statistically significant trends ( $\alpha = 0.1$ ). Background pattern represents regional trend. Blue indicates increasing flood discharges, red decreasing flood discharges. Rectangles indicate hotspot areas as in Fig. 2, Extended Data Fig. 3 and Extended Data Table 2c. (b) Uncertainties of the trends in terms of standard deviation. Points show local uncertainties. Background pattern represents regional uncertainties at the scale of a block size of 200 x 200 km. Units of both panels are % of mean/decade.



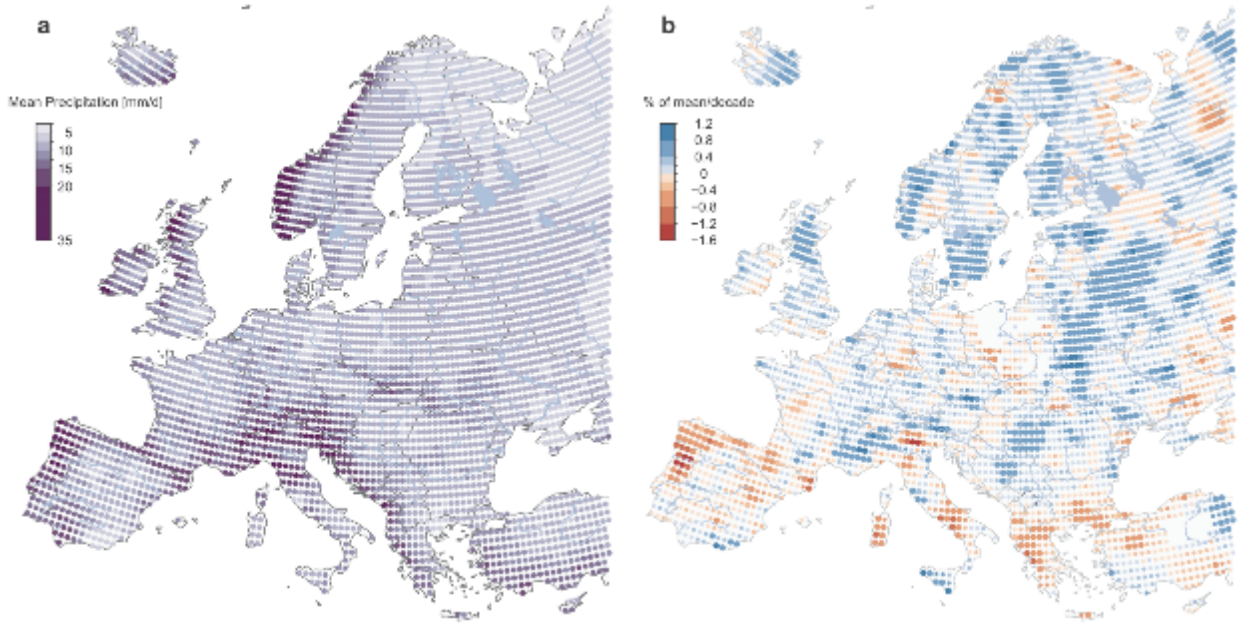
526  
 527  
 528  
 529  
 530  
 531  
 532

**Extended Data Figure 3 | Flood trends as in Fig. 1 and Extended Data Figure 2, but using fewer stations.**  
 (a) Only stations with significant trends are used (n = 664). (b) Only stations with distances from each other larger than 50 km are used (n = 745).



534  
 535  
 536  
 537  
 538  
 539  
 540  
 541  
 542

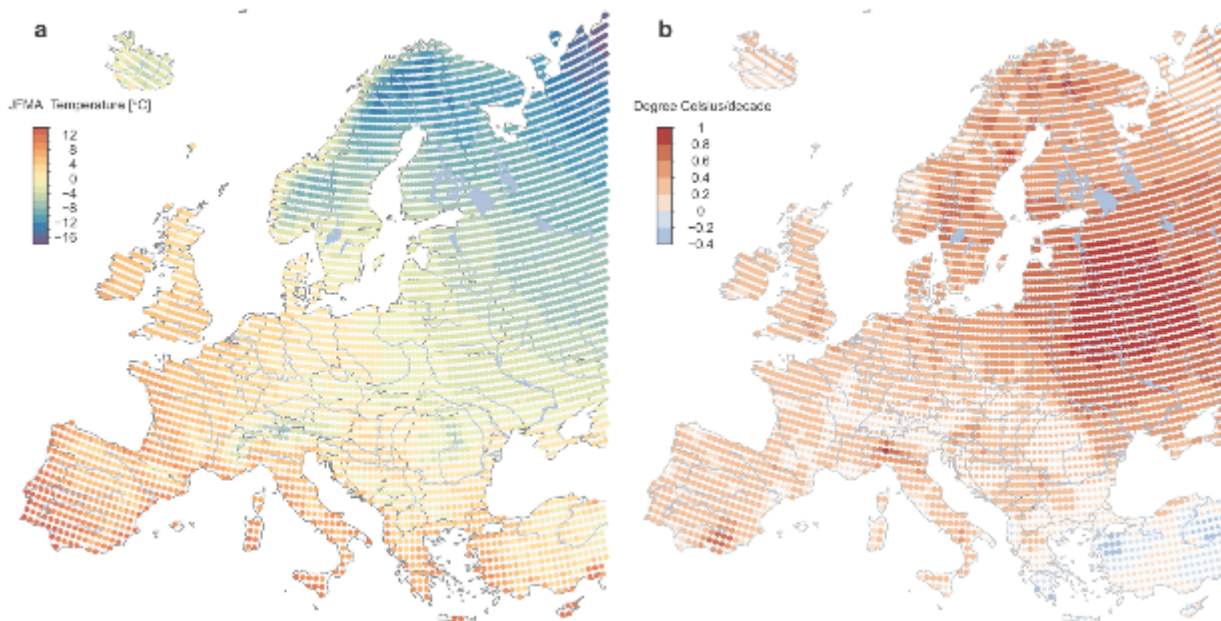
**Extended Data Figure 4 | Long-term temporal evolution of timing of floods and their drivers for seven hotspots in Europe.** (a) Northern UK, (b) Western France, (c) Southern Germany and Western Czechia, (d) Northern Iberia, (e) Central Balkans, (f) Southern Finland, (g) Western Russia. Timing of observed floods (green), 7-day maximum precipitation (purple), snowmelt index (orange), and maximum monthly soil moisture (blue). Lines show median timing and shaded bands indicate variability of timing within the year ( $\pm 0.5$  circular standard deviations). All data were subjected to a circular 10-year moving average filter. Vertical axes show month of the year (June to May).



543  
 544  
 545 **Extended Data Figure 5 | 7-day maximum precipitation (1960-2010).** (a) Long-term mean (mm/d); (b)  
 546 trends in precipitation (% of mean per decade), where larger points indicate statistically significant trends ( $\alpha =$   
 547 0.1); blue indicates increasing precipitation, red decreasing precipitation.  
 548  
 549



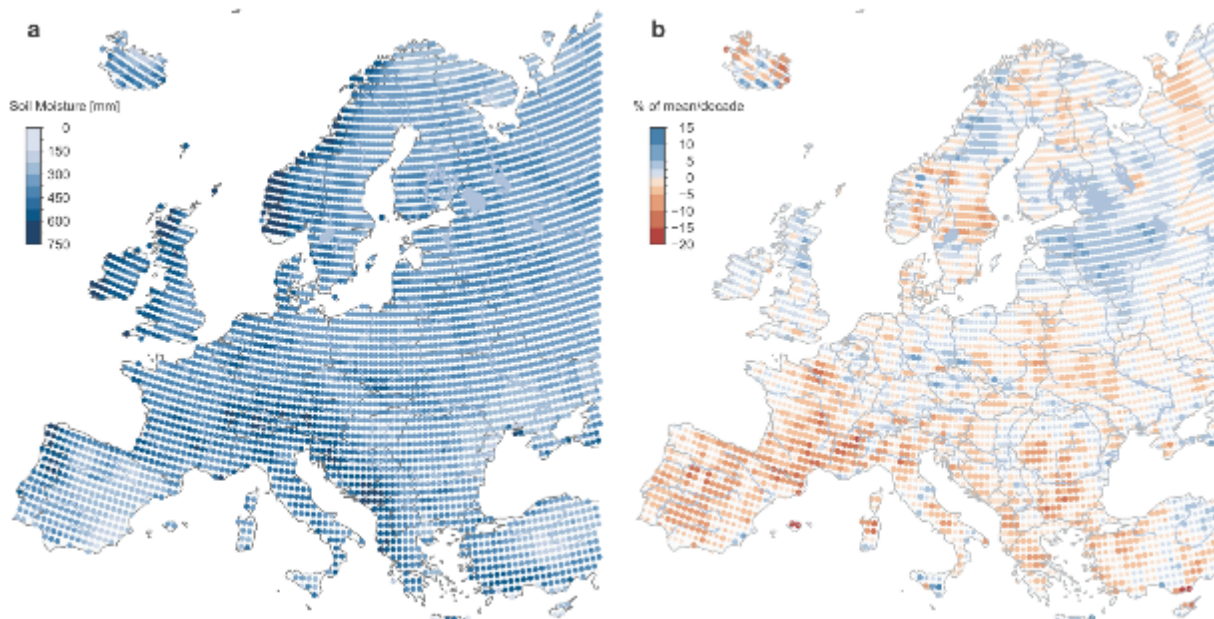
550  
551



552  
553  
554  
555  
556

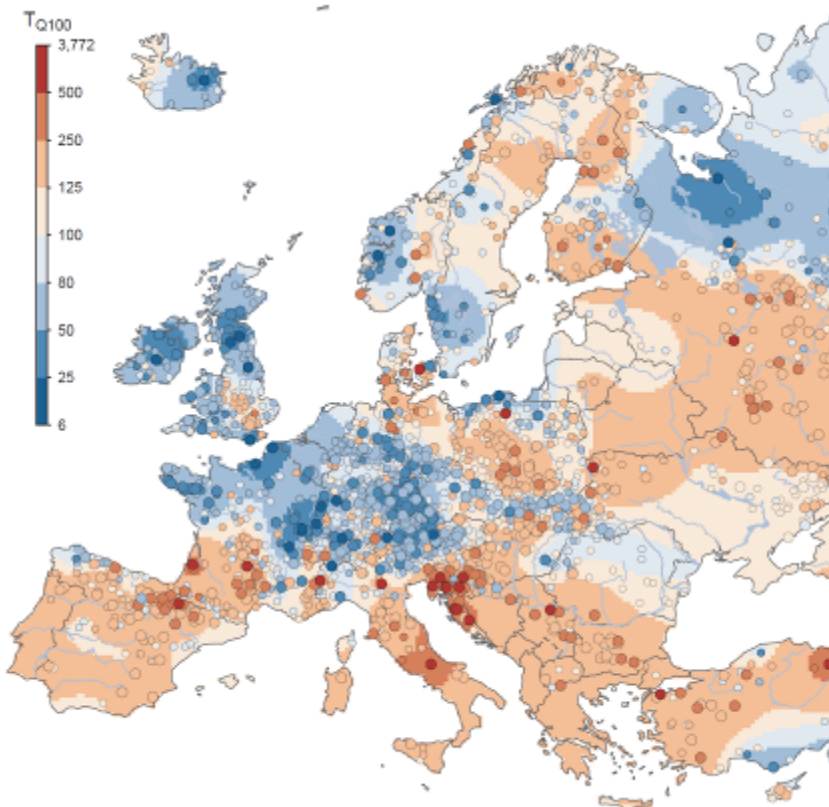
**Extended Data Figure 6 | Spring (January to April) mean air temperatures (1960–2010).** (a) Long-term mean (°C); (b) trends in temperatures (°C per decade), where larger points indicate statistically significant trends ( $\alpha = 0.1$ ); red indicates increasing temperature, blue decreasing temperature.

557  
558



559  
560  
561  
562  
563

**Extended Data Figure 7 | Annual maximum monthly soil moisture (1960–2010).** (a) long-term mean (mm); (b) trends in maximum soil moisture (% of mean per decade), where larger points indicate statistically significant trends ( $\alpha = 0.1$ ); blue indicates increasing soil moisture, red decreasing soil moisture.



565  
 566  
 567  
 568  
 569  
 570  
 571  
 572  
 573

**Extended Data Figure 8 | Estimated return period in 2010 of the discharge that was the 100-year flood in 1960.** Points show local return periods ( $n = 2370$ ), where larger points indicate agreement of the 5<sup>th</sup> and the 95<sup>th</sup> percentiles of the uncertainty distribution in the sign of change. Background pattern represents regional return periods. Blue indicates lower return periods representing increasing flood discharges, red indicates higher return periods representing decreasing flood discharges. This figure provides a continental overview, and does not replace national-scale and local studies where more detailed information may be available.

**Extended Data Table 1 | Data Sources contained in the European Flood Research Database.**

Country/Project	Data Holder/Source/Project information
Albania	National Hydro-Meteorological Service Albania, Institute of GeoSciences, Energy, Water and Environment (IGEWE)
Austria	Hydrographic Services of Austria (HZB)
Bosnia and Herzegovina	Hydrological Yearbooks of the former Republic of Yugoslavia
Bulgaria	Hydrological Yearbooks of the Rivers in Bulgaria, National Institute of Meteorology and Hydrology
Croatia	Meteorological and Hydrological Service of Croatia
Czechia	Czech Hydrometeorological Institute
Denmark	Danish Centre for Environment and Energy (DCE)
Estonia	Estonian Environment Agency
EWA	European Water Archive (EWA)
Finland	Finnish Environment Institute, Open information/Hydrology/Discharge, Source: SYKE
France	HYDRO database, French Ministry of Ecology, Sustainable Development and Energy
Germany	Federal Waterways and Shipping Administration (WSV)
Germany, Baden-Wuerttemberg	Ministry for the Environment, Climate and Energy of the Federal State of Baden-Wuerttemberg (LUBW)
Germany, Bavaria	Flood Information Centre, Bavarian Environment Agency, Munich (LfU)
Germany, Brandenburg	Ministry of Rural Development, Environment and Agriculture of the Federal State of Brandenburg (MLUL)
Germany, Hessa	Hessian Agency for Nature Conservation, Environment and Geology (HLNUG)
Germany, Lower Saxony	Lower Saxony Water Management, Coastal Defence and Nature Conservation Agency (NLWKN)
Germany, Mecklenburg-Western Pomerania	State Office of Environment, Nature Protection and Geology of Mecklenburg-Western Pomerania (LUNG)
Germany, North Rhine-Westphalia	State Agency for Nature, Environment and Consumer Protection (LANUV)
Germany, Rhineland-Palatinate	State Office for the Environment, Water Management and Commerce Inspectorate Rhineland-Palatinate (LUWG)
Germany, Saarland	The Saarland State Office for Environmental and Labour Protection (LUA)
Germany, Saxony	Saxon State Agency for Environment, Agriculture and Geology (LfULG)
Germany, Saxony-Anhalt	State Agency for Flood Defence and Water Management of Saxony-Anhalt (LHW)
Germany, Schleswig-Holstein	Schleswig-Holstein Agency for Coastal Defence, National Park and Marine Conservation (LKN.SH)
Germany, Thuringia	Thuringian Regional Office for the Environment and Geology (TLUG)
GRDC	The Global Runoff Data Centre, Koblenz, Germany
Greece	National Data Bank of Hydrological & Meteorological Information (NDBHMI)
Hungary	General Directorate of Water Management, Hungary
HYDRATE	EU-FP7 HYDRATE Project data base: Hydrometeorological Data Resources and Technology for Effective Flash Flood Forecasting
Iceland	Icelandic Meteorological Office, Hydrological Database, No. 2013-10-27/01
Ireland	Irish Environmental Protection Agency (EPA)
Ireland	Office of Public Works (OPW)
Italy	CUBIST database, former SIMN (Servizio Idrografico e Mareografico Nazionale)
Italy	National Research Council - Consiglio Nazionale delle Ricerche (CNR)
Italy	ENEL (Ente Nazionale per l'Energia Elettrica)
Italy	AdBPo (Autorità di Bacino del Fiume Po)
Italy	IRPI (Istituto di Ricerca per la Protezione Idrogeologica)
Italy	ISPRA (Istituto Superiore per la Protezione e la Ricerca Ambientale)
Italy, Emilia-Romagna Region	ARPA (Agenzia Regionale per la Protezione dell' Ambiente) Emilia-Romagna
Italy, Piedmont Region	ARPA Piemonte
Italy, Lazio Region	Ufficio Idrografico e Mareografico di Roma - Regione Lazio
Italy, Sicily Region	Osservatorio delle Acque della Regione Siciliana
Italy, South Tyrol Region	Hydrographic Office, Autonomous Province of Bolzano
Italy, Trentino Region	Dipartimento Protezione Civile, Provincia Autonoma di Trento
Italy, Umbria Region	Ufficio Idrografico - Regione Umbria
Italy, Veneto Region	ARPA Veneto
Latvia	Latvian Environment, Geology and Meteorology Centre, State Ltd.
Lithuania	Lithuanian Hydrometeorological Service
Macedonia	Macedonian Hydrometeorological Service
Netherlands	Rijkswaterstaat - Dutch Ministry of Infrastructure and the Environment
Norway	Norwegian Water Resources and Energy Directorate - Norges vassdrags- og energidirektorat (NVE)
Poland	Institute of Meteorology and Water Management National Research Institute (IMGW-PIB)
Portugal	Portuguese Environmental Agency - Agência Portuguesa do Ambiente, National Information System for Water Resources of Portugal (SNIRH)
Romania	National Institute of Hydrology and Water Management - NIHWMM
Russia	The main hydrological characteristics, 1963-1970, 1971-75, 1975-1980, 1980-2000
Russia	Ministry of Natural Resources and Ecology of the Russian Federation, State Hydrological Institute
Russia	State Water Cadastre, 1985-2010, State Hydrological Institute, Lomonosov Moscow State University
Russia	Automated information system of state water bodies monitoring (AIS GMVO), Federal Agency for Water Resources
Serbia	Republic Hydrometeorological Service of Serbia (RHSS), Hydrological Yearbooks of Surface Water, Belgrade
Slovakia	Slovak Hydrometeorological Institute (SHMI)
Slovenia	Slovenian Environment Agency (ARSO)
Spain	Centre for Hydrographic Studies (Centro de Estudios Hidrográficos) of CEDEX, Spain
Sweden	Swedish Meteorological and Hydrological Institute (SMHI)
Switzerland	Federal Office for the Environment (FOEN) / (BAFU)
Turkey	General Directorate of Electrical Power Resources Survey and Development Administration (EIE), Turkey
Ukraine	Hydrological Department, Ukrainian Hydrometeorological Institute (UHMI)
Ukraine	Hydrometeorological Institute, Odessa State Environmental University (OSENSU)
United Kingdom	UK National River Flow Archive (NRFA)



578  
579  
580

**Extended Data Table 2a | Number of stations with positive and negative flood discharge trends. Regions according to Fig. 1.**

		Positive Trend	Negative Trend	All
Europe	Significant $\alpha=0.1$	273 (11.52%)	391 (16.50%)	664 (28.02%)
	Not Significant	833 (35.15%)	837 (35.31%)	1706 (71.98%)*
	All	1106 (46.67%)	1228 (51.81%)	2370*
Region 1: North-western Europe	Significant $\alpha=0.1$	182 (20.34%)	27 (3.01%)	209 (23.35%)
	Not Significant	435 (48.60%)	240 (26.82%)	686 (76.65%)*
	All	617 (68.94%)	267 (29.83%)	895*
Region 2: Southern Europe	Significant $\alpha=0.1$	13 (2.84%)	142 (31.00%)	155 (33.84%)
	Not Significant	96 (20.96%)	169 (42.80%)	303 (66.16%)*
	All	109 (23.80%)	338 (73.80%)	458*
Region 3: Eastern Europe	Significant $\alpha=0.1$	5 (1.77%)	115 (40.78%)	120 (42.55%)
	Not Significant	54 (19.15%)	104 (36.88%)	162 (57.45%)*
	All	59 (20.92%)	219 (77.66%)	282*

[\*stations with no trend included]

581  
582  
583  
584  
585  
586

**Extended Data Table 2b | Estimates and 90% confidence bounds (in brackets) of Spearman's rank correlation coefficient ( $r$ ) between hotspot medians of the annual series of flood discharge and their drivers.**

	Northern UK	Western France	Germany Czechia	Northern Iberia	Central Balkans	Southern Finland	Western Russia
Precipitation	0.70** (0.57, 0.76)	0.41* (0.15, 0.64)	0.40* (0.24, 0.56)	0.54** (0.39, 0.68)	0.22 (-0.11, 0.49)	0.08 (-0.11, 0.28)	-0.13 (-0.4, 0.18)
Soil Moisture	0.36* (-0.01, 0.66)	0.57** (0.39, 0.71)	0.56** (0.41, 0.68)	0.37* (0.12, 0.55)	0.68** (0.50, 0.76)	0.20 (0.01, 0.4)	0.30 (0.07, 0.49)
Spring temperature	0.09 (-0.15, 0.25)	0.5** (0.33, 0.63)	0.04 (-0.19, 0.23)	0.02 (-0.23, 0.32)	-0.29 (-0.44, -0.12)	-0.34 (-0.49, -0.15)	-0.55** (-0.7, -0.3)

[(\*\*)  $p$ -value < 0.001, (\*)  $p$ -value < 0.01]

587  
588  
589  
590  
591  
592

**Extended Data Table 2c | Flood discharge trends for selected hotspots (as % of station mean per decade). The significance level of the general hotspot trends is given according to the Regional Mann-Kendall test<sup>38</sup> with significance level  $\alpha$ .**

Hotspot Name	No. of Stations	Minimum trend	Maximum trend	Mean hotspot trend	Significance
Northern UK	15	2.9	12.5	6.6	$\alpha < 0.01$
Western France	16	5.9	17.6	9.7	$\alpha < 0.01$
Germany Czechia	47	1.6	17.8	8.0	$\alpha < 0.01$
Northern Iberia	34	-18.3	3.8	-8.3	$\alpha < 0.01$
Central Balkans	15	-17.6	-0.1	-8.4	$\alpha < 0.01$
Southern Finland	15	-10.0	-2.1	-5.2	$\alpha < 0.01$
Western Russia	21	-28.8	-8.3	-18.2	$\alpha < 0.01$

593  
594  
595  
596